J Fluoresc (2007) 17:739–748
DOI 10.1007/s10895-007-0185-1

ORIGINAL PAPER

An Ensemble and Single-molecule Fluorescence Spectroscopy Investigation of Calcium Green 1, a Calcium-ion Sensor

Yin Lu · Matthew F. Paige

Received: 29 January 2007 / Accepted: 19 March 2007 / Published online: 20 July 2007

Abstract The calcium-ion indicator dye, Calcium Green 1 (CG-1), has been characterized using a combination of ensemble and single-molecule optical spectroscopy measurements. In terms of ensemble measurements, CG-1 demonstrated a strong increase in fluorescence emission as a function of increasing [Ca^{2+}]. This was accompanied by a change in the relative proportions of two chemical forms of the dye, each with a different fluorescence lifetime, which were found to co-exist in solution. From single-molecule fluorescence measurements, it was found that the fluorescence intensity and photobleaching time (on-time) of each CG-1 molecule was invariant with [Ca^{2+}] and that changes in ensemble fluorescence intensity simply correlates with the number of fluorescent molecules in solution. These results are compared with that of the related system, Calcium Green 2 (CG-2), and the mechanisms of operation of these two indicator dyes are discussed.

Keywords Fluorescence · Spectroscopy · Single-molecule · Calcium-ion · Sensor

Introduction

Single-molecule (SM) spectroscopy is a young but rapidly-developing field of research in which the optical properties of individual, isolated molecules can be probed in the absence of ensemble averaging [1–4]. The SM approach to optical spectroscopy has now been applied to a host of systems, ranging from single impurity atoms in crystals, to complex biological systems and beyond. Fluorescence emission of individual molecules can be an extremely sensitive probe of local environmental conditions, and has provided valuable insight into the heterogeneous nature of numerous systems. While interesting in and of themselves, one of the major practical benefits of spectroscopic measurements on individual molecules is that they can provide invaluable complementary information to more conventional ensemble spectroscopy measurements. While not yet routine, it is conceivable that SM measurements might soon become a standard tool when characterizing novel new fluorophores and photophysical processes.

Of recent interest to our research group has been the application of SM spectroscopy for characterizing luminescent ion-indicator molecules, chemical entities that undergo significant changes in fluorescence emission upon binding with inorganic ions. The design, synthesis and characterization of a huge number of different ion-indicators has been reported in the literature (for a number of important reviews, see [5–9]). Indicators have been developed to detect different types of ions, to emit over a wide range of emission wavelengths and to operate through a variety of signal transduction mechanisms. Ion-indicators have found numerous applications, including detection and quantification of harmful inorganic analytes in environmental analysis, as well as to visualize, through high-sensitivity fluorescence imaging, localized ion-dependent processes in live cells and tissues.

SM measurements have been applied to a number of important ion-sensor systems. For example, Adams et al. have reported the synthesis and characterization of a novel perylene-based sensor that can detect binding events at the single-molecule level via a photoinduced electron transfer (PET) mechanism [10]. Brasselet et al. have described the

Y. Lu · M. F. Paige (✉)
Department of Chemistry, University of Saskatchewan,
110 Science Place, Saskatoon, SK S7N 5C9, Canada
e-mail: matthew.paige@usask.ca

fluorescence behaviour of the seminaphtorhodafluor SNARF-1 for pH sensing in agarose matrices [11], as well as the use of a "cameleon" protein construct to detect Ca^{2+} binding [12]. While not directly attempting to produce an indicator-ion system, Ha et al. [13] demonstrated changes in energy transfer between fluorescently labeled components of an RNA assembly upon Mg^{2+} binding.

Fluorescence-based ion-indicators that can be used to detect Ca^{2+} are arguably the most important and widely used types of indicators because of the great importance of intracellular Ca^{2+} in biological signaling pathways [14, 15]. These indicators are used routinely in fluorescence microscopy experiments, in which the indicator fluorescence is used to directly visualize the presence of Ca^{2+} in tissues or cells. Many varieties of these ion-indicators have been developed, and indeed many are now commercially available. We have recently reported a combined ensemble and single-molecule investigation of Calcium Green 2 (CG-2), a commercially available calcium-ion indicator that exhibits a large increase in fluorescence emission intensity upon binding Ca^{2+} [16]. The Calcium Green class of indicators are based upon the calcium-chelating ligand 1,2 bis(o-aminophenoxy)ethane-N,N,N′N′-tetracetic acid (BAPTA) [17]. The BAPTA moiety has excellent Ca^{2+} binding properties, including a low dissociation constant, high selectivity and rapid substrate binding. By coupling BAPTA to a xanthene (rhodamine-based) fluorophore, sensors that become highly fluorescent in the visible region of the spectrum have been developed [18–21]. The Calcium Green class of indicators consists of a single BAPTA moiety combined with either one (CG-1) or two (CG-2) rhodamine-based fluorophores. These indicators have low calcium dissociation constants (manufacturer lists K_d values of 0.19 μM and 0.55 μM, for CG-1 and CG-2, respectively) and high quantum yields (0.75 in high [Ca^{2+}]) at physiological pHs. Structures of CG-1 and CG-2 are shown in Fig. 1a,b.

While the mechanism by which signal transduction occurs in some ion-indicators is well known, this was not the case for CG-2. In our previous work, a combination of optical spectroscopy measurements was used to determine why the molecule becomes strongly fluorescent on Ca^{2+} binding [16]. It was found that in the absence of Ca^{2+}, CG-2 adopts a conformation in which the transition dipoles for the two fluorophores are coplanar. This gives rise to intramolecular exciton formation and a corresponding "self-quenching" of fluorescence emission. When the molecule binds to Ca^{2+}, the relative separation and orientation of the constituent fluorophores are shifted, a large increase in fluorescence emission intensity is observed and an accompanying shift in CG-2's absorption spectrum takes place. This suggests that upon binding of Ca^{2+}, the intermolecular exciton formation for this system is disrupted.

From complementary SM experiments, it was observed that the change in bulk fluorescence correlated with a simple statistical increase in the number of fluorescent molecules in solution, as anticipated from ensemble measurements. In addition, it was also found that the majority of CG-2 molecules photobleached in a single step (collective photobleaching), despite the presence of two fluorophores per molecule. This provided an excellent opportunity to investigate collective photobleaching, a well-known phenomenon in multi-flurophore systems, in a comparatively simple and controllable test-system. It was postulated that for CG-2, collective photobleaching could be attributed to rapid dipole-dipole Förster coupling between the two fluorophores in conjunction with the formation of a photodamaged induced trap site on one of the fluorophores.

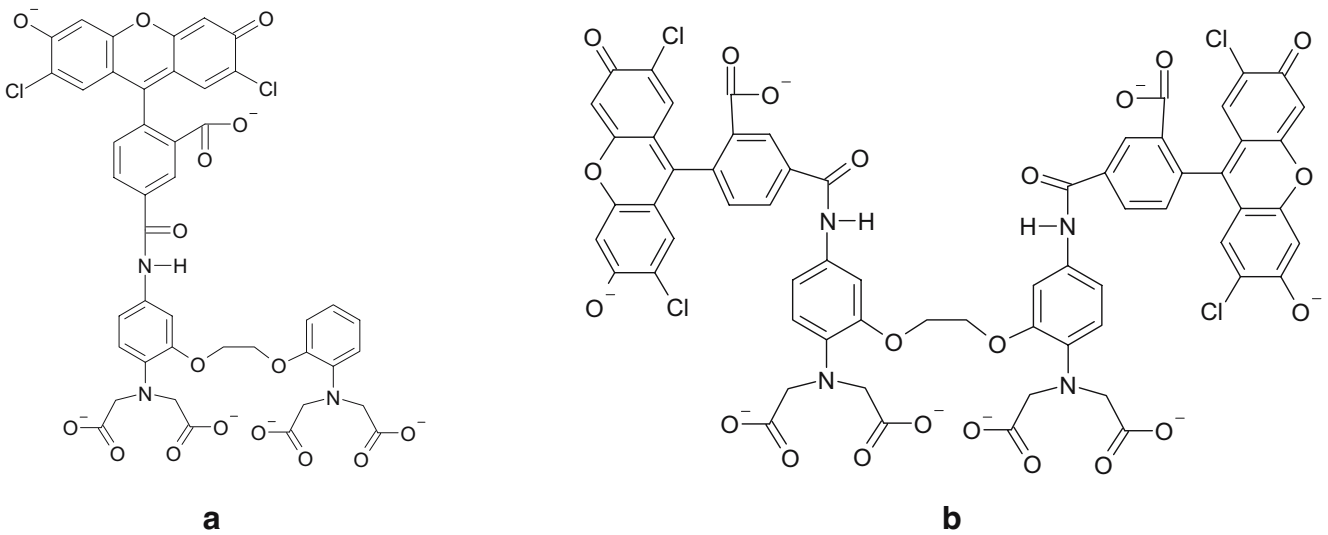

Fig. 1 Chemical structures for **a** Calcium Green 1 and **b** Calcium Green 2

The mechanism of action of CG-1 and a number of closely-related compounds has been shown by de Silva et al. [22] to be PET, in which rapid electron transfer from the Ca^{2+} binding domain donor to the photoexcited fluorophore acceptor takes place and renders it non-fluorescent. Upon Ca^{2+} binding, the PET process is retarded (the oxidation potential of the binding domain shifts significantly upon Ca^{2+} uptake) and fluorescence is re-activated. It is anticipated that while there will be some similarities between CG-1 and CG-2 in terms of basic spectroscopic properties, differences between the two will provide further useful insight into the mechanism of operation of both dyes. For example, the nature of the excitonic "quenched" state in CG-2 should be readily distinguishable through comparison of absorption spectra for the two molecules. One might also reasonably expect to distinguish between CG-1 and CG-2 at the single-molecule level by simply comparing mean fluorescence intensity levels. In this paper, we present a combined ensemble and SM spectroscopic characterization of CG-1 and compare these findings with those obtained previously for CG-2.

Materials and methods

Ensemble spectroscopy measurements

CG-1, CG-1 conjugated dextran, CG-2 and calcium buffers that contain a well-defined concentration of free Ca^{2+} (not chelated, referred to as $Ca^{2+}{}_{free}$) were obtained from Invitrogen Inc. (Burlington, ON, Canada) and used as received. For ensemble measurement, stock solutions of indicators were prepared by dissolving the bulk solid in pH 7.2 Tris buffer. Immediately before taking spectroscopic measurements, aliquots of the stock solution were added to an appropriate $Ca^{2+}{}_{free}$ buffer. Absorption and emission spectra were collected in quartz cuvettes on a Varian Cary 500 UV-Vis spectrophotometer and a SPEX 212 spectrofluorimeter, respectively. Fluorescence lifetimes were measured using the method of time-correlated single-photon counting (TCSPC), on a system described in detail elsewhere [16]. Excitation was performed at 488 nm, with the emission collection wavelength of 536 nm. Fluorescence decay profiles were fit using a non-linear least squares reconvolution procedure based on the Marquardt algorithm. The quality of fit was assessed through the value of the reduced χ^2 and through the distribution of weighted residuals.

Single-molecule fluorescence spectroscopy measurements

Single-molecule fluorescence measurements were carried out using a home-built, wide-field epifluorescence microscope [23]. Samples were excited with circularly polarized, continuous wave light from a tunable argon-ion laser, with a wavelength of either 488 or 514 nm (see subsequent text for details). Excitation intensities were typically in the range of 0.5–2.0 kW/cm^2, as measured by dividing the incident power measured at the sample focal plane by the illumination area. Samples were prepared in either one of two ways. In the first approach, an aliquot of a dilute polymer (2% w/v poly(vinyl alcohol) in Millipore water) was spin-cast onto a clean microscope coverglass slide, followed by a dilute solution (~10^{-9} M) of indicator dye in an appropriate $Ca^{2+}{}_{free\ buffer}$. In the second approach, a dilute solution of CG-1 conjugated dextran in Ca^{2+} buffer was mixed with melted, low-gelling temperature agarose (Sigma-Aldrich) which had been prepared using Ca^{2+} calibration buffers. The dye-doped agarose was then sandwiched between two clean pieces of coverglass and allowed to cool. Control samples with the absence of dye show no fluorescent impurities when examined under single-molecule imaging conditions. The use of dextran conjugated CG-1 prevented translational diffusion of the dye through the water-filled pores of the agarose matrix, a phenomenon that has been observed previously in other single-molecule investigations that made use of gels as a support medium [24, 25]. We found that, other than slightly different background signal levels, the two sample preparation approaches gave comparable results in terms of single-molecule measurements.

Results and discussion

Ensemble spectroscopy measurements

When fluorescence excitation was carried out at 488 nm, the emission spectrum of CG-1 consisted of a single peak with emission maximum at 534 nm. Addition of Ca^{2+} to CG-1 resulted in an increase in the overall emission intensity of the indicator dye solution. Figure 2 shows a series of fluorescence emission spectra in which the $[Ca^{2+}]_{free}$ was systematically varied over a concentration range of 0–1.35 μM. There was no substantial shift in peak positions observed with increasing $[Ca^{2+}]_{free}$, but rather a simple increase in the overall fluorescence intensity. Above $[Ca^{2+}]$ of 1.35 μM, there was no further increase in emission intensity with further addition of calcium, indicating saturation of CG-1 had occurred.

By assuming CG-1 binding can be modeled as a simple two-state equilibrium binding process in which the calcium free form of the indicator is non-fluorescent, one can derive Eq. 1:

$$\log\left(\frac{F_x - F_{\min}}{F_{\max} - F_x}\right) = n\log\left[Ca^{2+}\right] - \log K_d \quad (1)$$

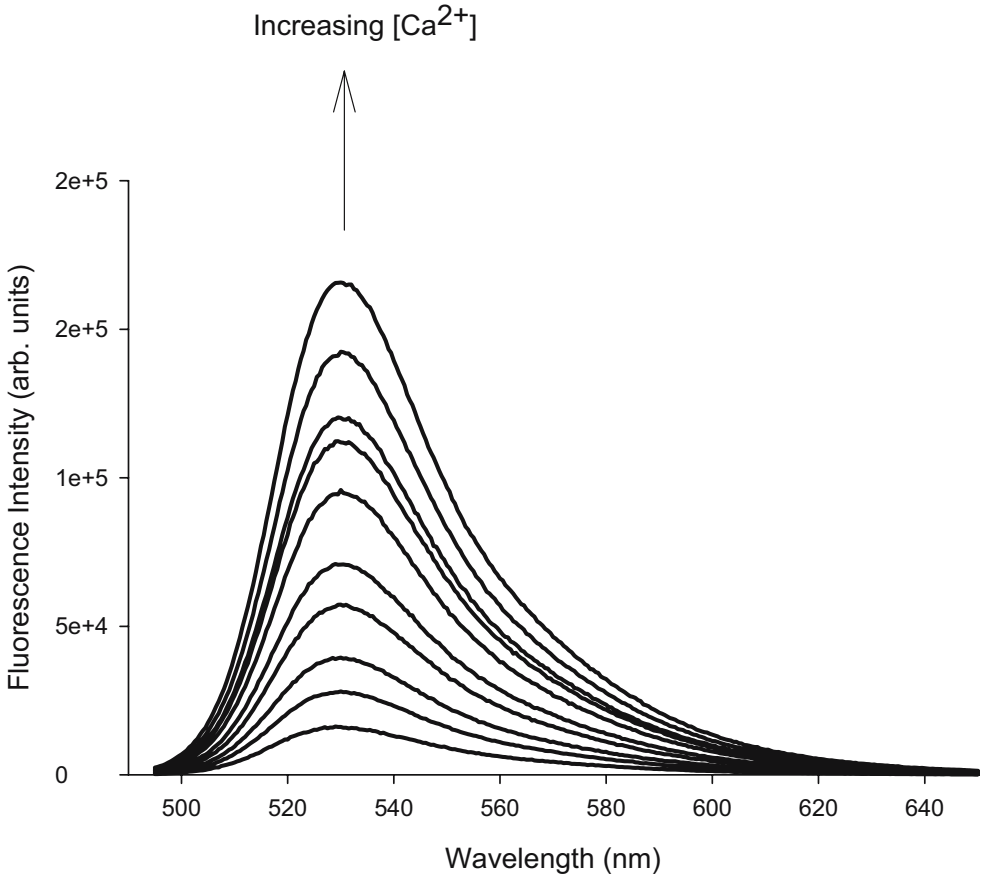

Fig. 2 Fluorescence emission spectra showing the change in emission of CG-1 as a function of increasing $[Ca^{2+}]_{free}$ ($[Ca^{2+}]_{free}$ ranges from 0 to 1.35 μM, [CG-1]=1.50 μM)

where F_x, F_{min} and F_{max} are the fluorescent intensities corresponding to the $[Ca^{2+}]_{free}$ of interest, the intensity at $[Ca^{2+}]_{free}=0$ and the intensity measured at the maximum value of $[Ca^{2+}]_{free}$, K_d is the dissociation constant for the CG-1·$[Ca^{2+}]$ complex and n is the binding stoichiometry. From the emission data, a K_d of 0.21 μM was calculated, which is in excellent agreement with the value of 0.19 μM reported by the manufacturer [17], along with a 1:1 binding stoichiometry between the indicator and Ca^{2+}.

At saturating conditions of $[Ca^{2+}]_{free}$ (>1.35 μM), the total fluorescence emission intensity, as determined by measuring the integrated area under the emission spectra, increased 16-fold over that of the nominal calcium free buffer. For the calcium free buffer, the emission intensity was extremely low but not precisely zero. This is consistent with the previous measurements carried out on the CG-2 system. The likely sources of this residual fluorescence is trace amounts of unchelated Ca^{2+} in the system and weak fluorescence from uncomplexed CG-1. It is worth noting that the net change in fluorescence emission intensity for CG-1 is almost exactly half of the value that we have reported previously for the CG-2 system (38-fold over the calcium free buffer). This result is entirely consistent with the chemical structures of the two sensor dyes—one would anticipate an approximate doubling of the absorption cross-section of CG-2 over CG-1 simply because of the presence of the two fluorophores in the molecule, and hence a proportional increase in fluorescence output.

In addition to steady-state measurements, time-resolved (lifetime) fluorescence measurements have also been carried out on CG-1. Fluorescence lifetime decay curves, measured for samples ranging in $[Ca^{2+}]_{free}$ from zero to saturation, were well fit by a double-exponential decay (Eq. 2) in which none of the fitting parameters (lifetime or pre-exponential factors) were fixed.

$$I(t) = \alpha_1 e^{-t/\tau_1} + \alpha_2 e^{-t/\tau_2} \quad (2)$$

Curve fitting indicated the presence of two different lifetime components, a long-lived component with a lifetime of 3.4±0.1 ns and a short-lived component with lifetime of 0.2±0.1 ns. A typical fluorescence lifetime decay curve taken at $[Ca^{2+}]_{free}=0.605$ μM is shown in Fig. 3. The relative weighting of the two lifetime components, as determined by the pre-exponential factors (amplitudes), shifted as a function of $[Ca^{2+}]_{free}$. As the $[Ca^{2+}]_{free}$ increased, the pre-exponential factor of the long-lived component increased (0.05 at zero calcium levels, increasing

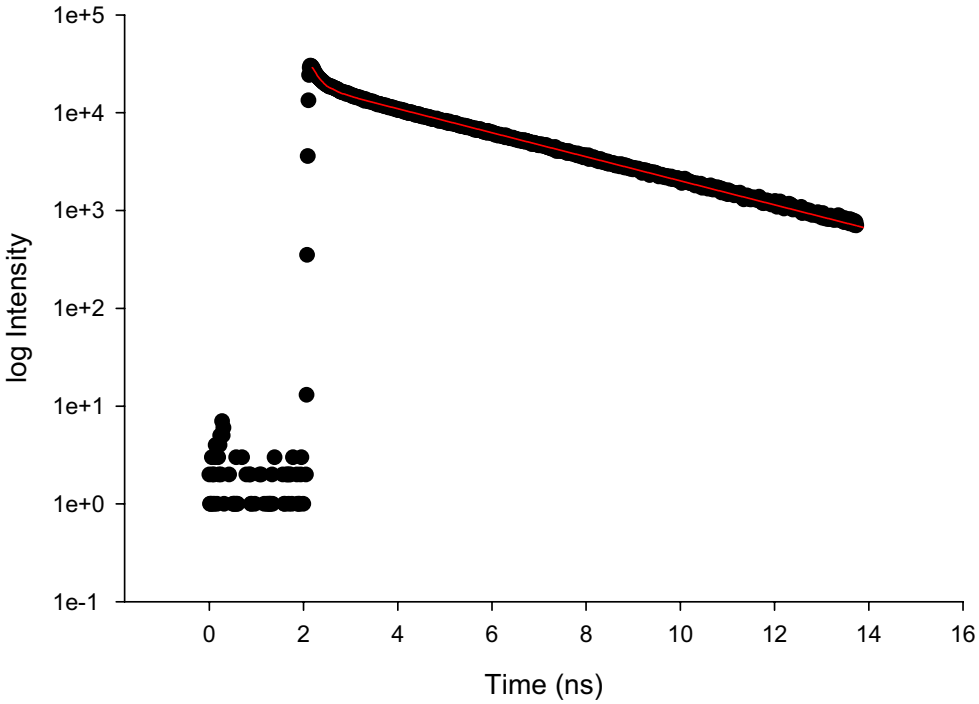

Fig. 3 Typical fluorescence life-time measurement taken from $[Ca^{2+}]_{free}$=0.602 μM. The *red line* is a double-exponential fit, as described in the main text body

to 0.62 at saturating levels of calcium) and the pre-exponential factor of the short-lived component correspondingly decreased.

For CG-1 we interpret this behaviour as being caused by the presence of two distinct chemical species in solution, with the long-lived component corresponding to the presence of the highly-fluorescent (Ca^{2+} bound) specie, and the short-lived component corresponding to the weakly-fluorescent Ca^{2+} free specie. Changes in the pre-exponential factors correspond to changes in the relative proportions of the two species in solution. Similar results for CG-1 lifetimes have been reported by Sanders et al. [26] during fluorescence lifetime imaging experiments on live cells, as well as by Tessier et al. in a fluorescence correlation spectroscopy characterization of conformational dynamics in the CG-1 system [27]. The behaviour and the values for fluorescence lifetimes that have been measured here for CG-1 are also comparable with those we have previously for the CG-2 system [16]. For CG-2, two different life-time components (3.5±0.1 and 0.3±0.1 ns) were also observed, with the pre-exponential factors changing in response to the $[Ca^{2+}]_{free}$. Again, it is not particularly surprising that there is excellent agreement between the lifetimes observed for CG-1 and CG-2, since the fluorophores, while differing in number, are structurally identical. While the mechanism that gives rise to the onset of fluorescence may differ between the two indicators, in both cases the end result of calcium binding is that the fluorophore becomes uncoupled from the rest of the molecule and behaves as an independent flurophore.

In addition to fluorescence spectroscopy characterization, absorption spectroscopy can also provide valuable insight into the nature of the CG-1 system. Figure 4 shows an absorption spectrum for CG-1 taken at zero $[Ca^{2+}]_{free}$. For comparison, this has been overlapped with the absorption spectrum for CG-2 taken under the same solution conditions. For CG-1, the spectrum consists of a strong peak with absorption maximum at 508 nm and a small shoulder around 460–470 nm. The relative sizes and positions of these spectral features were unaffected by the $[Ca^{2+}]_{free}$ over the entire range of concentrations used in the fluorescence measurements. This is in direct contrast with the behaviour that was reported previously for CG-2, which, at zero $[Ca^{2+}]_{free}$ has two strong peaks located at 490 and 508 nm. Upon increasing $[Ca^{2+}]_{free}$ in CG-2, the relative peak heights were found to shift in favour of the 508 nm peak, to the point where, at saturating concentrations, the blue-shifted shoulder could no longer be distinguished from the dominant red-shifted peak. In combination with force-field based conformational search calculations and fluorescence measurements, the blue-shifted peak was attributed to the formation of a fluorescently quenched exciton state, while the red-shifted peak was tentatively attributed to the two constituent fluorophores on CG-2 behaving as independent monomers resulting from the elimination of exciton splitting. While the previous argument was entirely consistent with the experimental data, an alternative interpretation of the spectra is that the red-shifted peak may be attributed to the formation of an additional excitonic state.

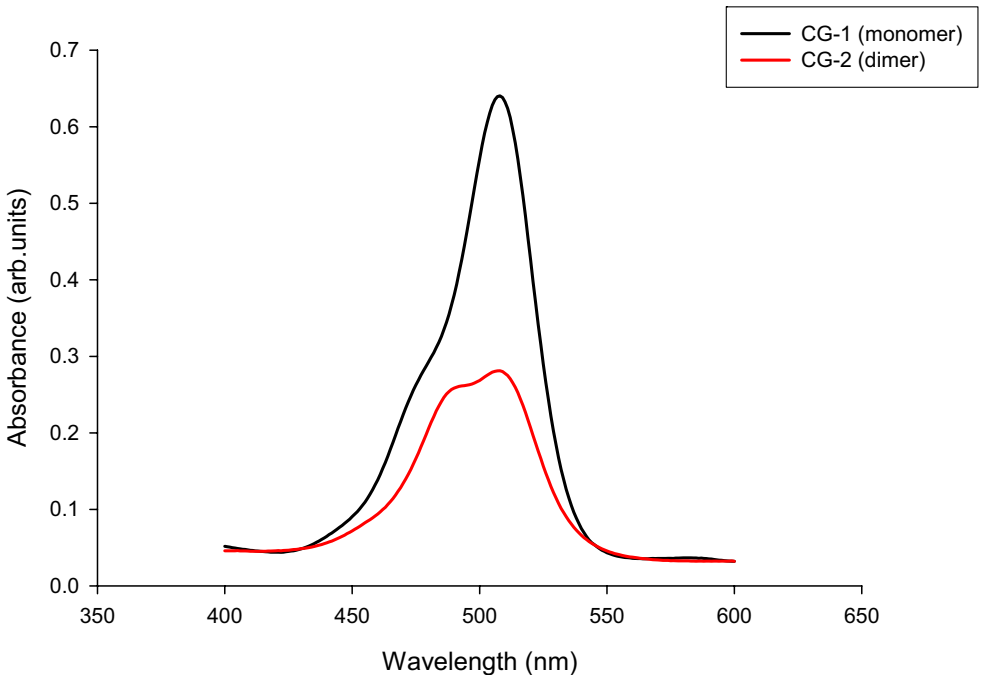

Fig. 4 Comparison of absorbance spectra for CG-1 and CG-2 at nominal $[Ca^{2+}]_{free}$=0 μM

By comparing the absorption spectrum of CG-1 with CG-2, one can definitively identify the nature of the red-shifted peak. Since this peak overlaps exactly with the absorption peak of the "monomeric" CG-1, one can attribute the red-shifted peak of CG-2 to the pure monomer. This additional measurement clearly shows that once CG-2 has bound Ca^{2+}, the two fluorophores no longer quench one another and behave as independent monomers. In the case of CG-1 which operates via a PET mechanism, no significant alterations in the absorption spectrum of the indicator as a function of $[Ca^{2+}]_{free}$ would be anticipated, which is in agreement with the experimental results obtained here.

Single-molecule fluorescence spectroscopy measurements

Preparation of samples as described in the "Materials and methods" gave rise to a series of bright, fluorescent spots when the samples were imaged in the fluorescence microscope. Under constant laser illumination, the fluores-

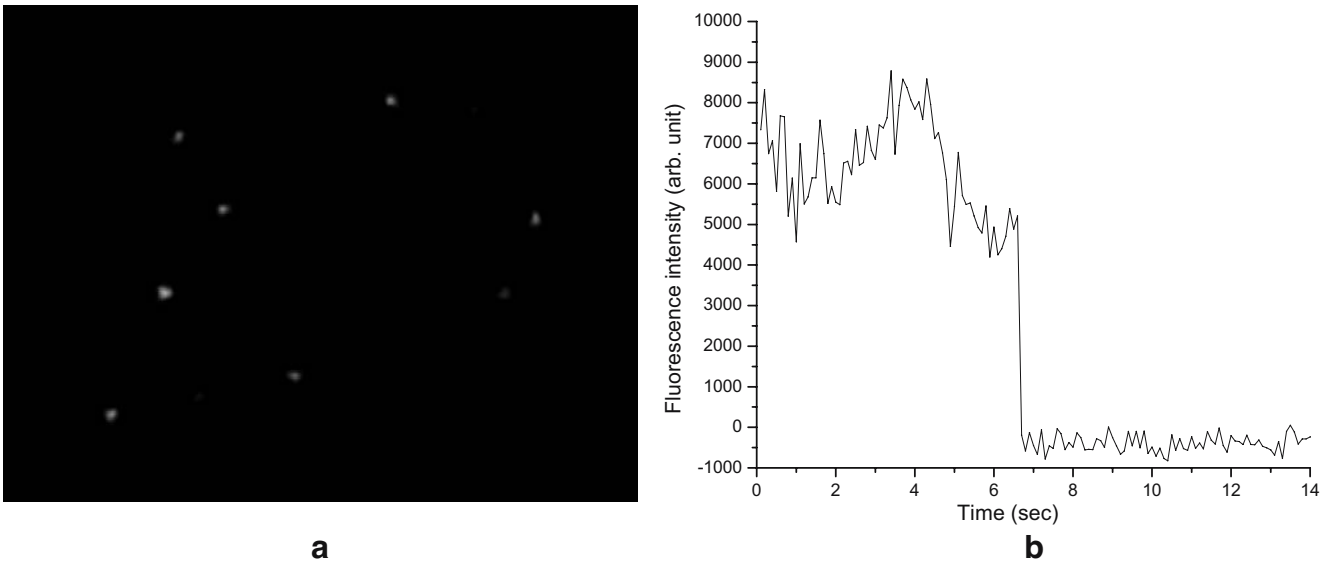

Fig. 5 **a** Fluorescence image of single CG-1 molecules (~10×12 μm) and **b** a typical single-molecule fluorescence time trajectory ([CG-1]=1×10^{-9} M, $[Ca^{2+}]_{free}$=5 μM , Excitation intensity=0.8 kW/cm^2)

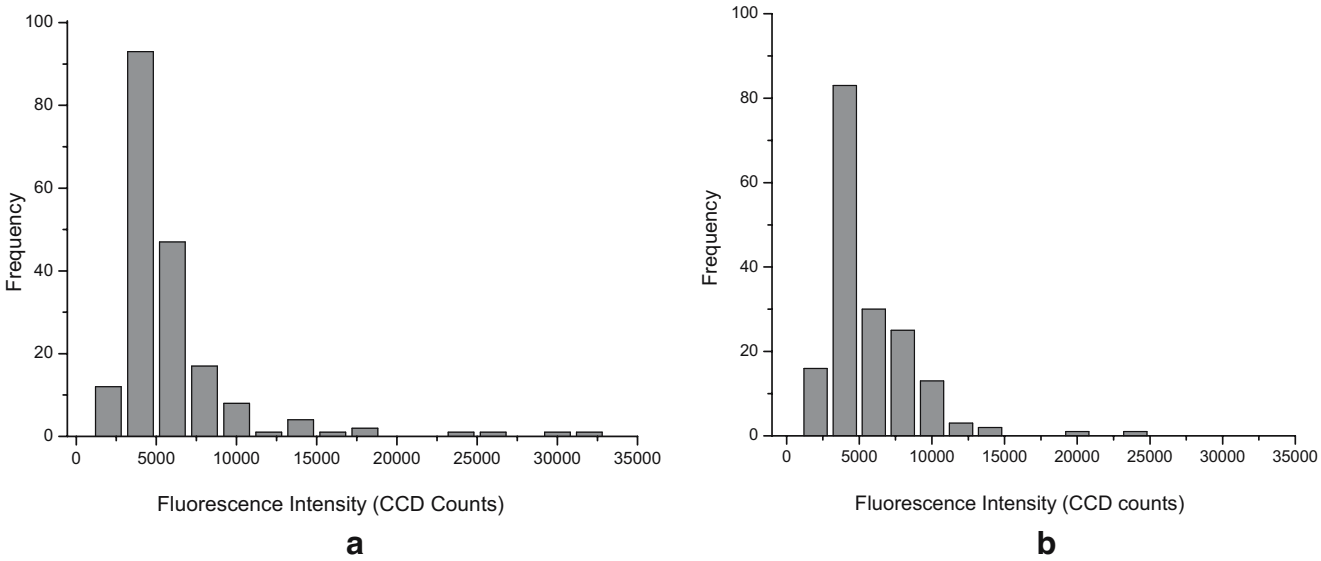

Fig. 6 Histograms of single-molecule fluorescence intensities for **a** $[Ca^{2+}]_{free}$=0 μM and **b** $[Ca^{2+}]_{free}$=5 μM. In both cases, excitation intensity was 0.8 kW/cm^2

cent spots underwent single-step photobleaching which is taken here, in combination with the diffraction-limited fluorescent spot size and low fluorophore concentration levels, as the signature of individual molecules. A typical fluorescence microscope image of single CG-1 molecules and a fluorescence time trajectory (fluorescence intensity of an individual molecule as a function of time) is shown in Fig. 5.

The fluorescence intensity of individual molecules of CG-1 was measured over $[Ca^{2+}]_{free}$ ranging from the nominal zero concentration to past the saturation level. Consistent with the ensemble fluorescence spectroscopy, samples prepared at $[Ca^{2+}]_{free}$= 0 were not entirely free of fluorescent entities. At zero calcium concentration individual fluorescent molecules could still be detected, though at nanomolar dye concentrations, their number density was very low. To make counting and analysis of these molecules easier, samples were prepared at a higher indicator dye concentration. Increasing the $[Ca^{2+}]_{free}$ resulted in a significant increase in the number of fluorescent molecules that could be detected, but did not affect the average fluorescence intensity of the molecules. Figure 6 shows two histograms of single-molecule fluorescence intensities (in CCD counts) taken at $[Ca^{2+}]_{free}$= 0 and at a $[Ca^{2+}]_{free}$ above saturation. The two histograms do not differ significantly from one another, and in view of this, we can attribute the general increase in fluorescence intensity of the dye solutions with a simple increase in the number of fluorescent molecules in solution which is as expected from the ensemble measurements. Indeed, samples prepared at saturating $[Ca^{2+}]_{free}$ can be prepared at lower indicator dye concentrations in order to achieve the same number density of molecules in the sample. We note that the fluorescent intensities of the individual CG-1 molecules are comparable with the emission intensities we have reported previously, under similar imaging conditions, for individual rhodamine 6G molecules [23], which is entirely reasonable given the nature of the fluorophore.

As an additional, simple verification that there were no significant changes in the spectroscopic nature of CG-1 molecules as a function of $[Ca^{2+}]_{free}$, histograms of photobleaching times (on-times) were measured for a number of different calcium concentrations. If the emission properties of CG-1 molecules are indeed independent of $[Ca^{2+}]_{free}$, then one would anticipate no significant differences in the mean photobleaching times measured as a function of concentration. Figure 7 shows on-time histograms for CG-1 taken at two extreme points of $[Ca^{2+}]_{free}$, one in the absence of calcium the other under saturating calcium concentrations. In both cases, the data was well fit by a single exponential function, as expected for a simple, random Poisson process [28]. Fitting constants were within one measure of standard error of each other, indicating that within the time resolution of our system, there was no significant difference in photobleaching time for the two different set of conditions. While these simple photobleaching experiments will not probe more subtle differences between fluorophores, it is reasonable to assume from the combination of these measurements and the SM intensity characterization, that there is no substantial difference between the spectroscopic properties of CG-1 as a function of $[Ca^{2+}]_{free}$.

During the course of their SM studies, both Ha et al. [13] and Brasselet et al. [11] noted statistically significant variations in the width of a variety of single-molecule

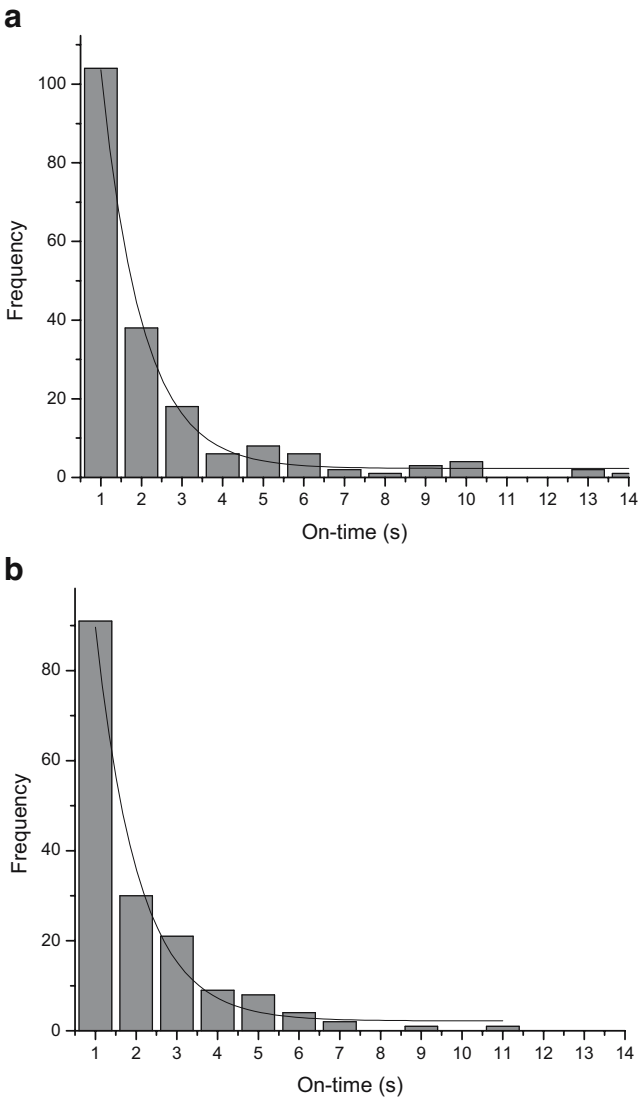

Fig. 7 Histogram of fluorescence on-times along with single-exponential fits (fitting equation was $f(x)=A_1 \exp(-x/t_1)+y_0$) for individual CG-1 molecules measured at **a** $[Ca^{2+}]_{free}=0$ μM ($t_1=1.00+0.05$ s^{-1}), **b** $[Ca^{2+}]_{free}=5$ μM ($t_1=1.05+0.11$ s^{-1}). In both cases, the laser excitation intensity was 0.8 kW/cm^2

measurement histograms as a function of target ion concentration. These width variations were tentatively attributed to a distribution of free energy changes for the deprotonation-protonation equilibrium related to local environmental effects. For Brasselet's pH sensor system, it was proposed that a possible source of variation in the local environment were interactions of the dextran chain (Brasselet et al. also made use of a dye-labeled dextran chain to minimize translational diffusion in agarose) with the wall of the agarose pores. For the CG-1 dextran system, these effects, if they exist, do not appear to significantly affect the observed SM histogram widths. However, since CG-1 binds its target ion much more strongly than the SNARF-1 pH sensor, it is reasonable to expect that effects related to binding and unbinding of the target ion would be negligible. In general, there is much information that could potentially be extracted from the shapes of histograms in SM experiments, and further efforts need to be devoted to this important aspect of data analysis in the future.

In addition to probing the nature of the CG-1 fluorophore and SM histogram widths, it is also informative to compare the relative intensities of individual CG-1 and CG-2 molecules. Figure 8 shows an overlay of two typical single-molecule fluorescence time trajectories for CG-1 and CG-2. It must be noted that in preliminary single-molecule measurements of CG-1, experiments were carried out under the same conditions as those used to characterize CG-2 (488 nm excitation, 0.9 kW/cm^2 excitation intensity, same emission filters and CCD multiplier gain) in order to allow direct comparison of experimental data. However, it was found that the CG-1 single-molecule emission intensity was significantly lower than that obtained for CG-2 with the same instrumental settings, and in order to produce acceptable signal-to-noise ratios, the excitation wavelength was adjusted to 514 nm (absorption maximum is 508 nm) and appropriate emission filters were selected. In general, it was observed that CG-2 molecules always had a significantly greater emission intensity than CG-1 molecules (typically ~9,000 CCD counts/100 ms for CG-2 versus ~4,500 CCD counts/100 ms for CG-1). While comparing absolute intensities in single-molecule measurements is often problematic because of the influence of randomly oriented transition dipoles and minor inhomogeneities in illumination intensity across the diameter of the epifluorescence illumination spot, it was found that CG-2 molecules had approximately twice the intensity of CG-1 molecules. Of course, the relative difference in excitation efficiency that comes from using 514 nm over 488 nm must be accounted for in this comparison, though this should lead to relatively minor (order one) corrections in the overall CG-1 intensity. It should also be noted that the emission filter sets used for 514 and 488 nm excitation had comparable transmission efficiencies over the emission range of CG-1, and will not substantially alter the overall signals.

Even accounting for the minor differences in excitation wavelength, the results of the single-molecule imaging experiments are consistent with those obtained from the bulk studies. That is, at the single-molecule level, CG-2 is approximately twice as bright as CG-1. Again, this is exactly the expected result. On a per molecule basis, the fluorescence signal of CG-2 should be approximately twice that of the monomeric CG-1, simply because the molecule will have an absorption cross-section that is approximately twice as large.

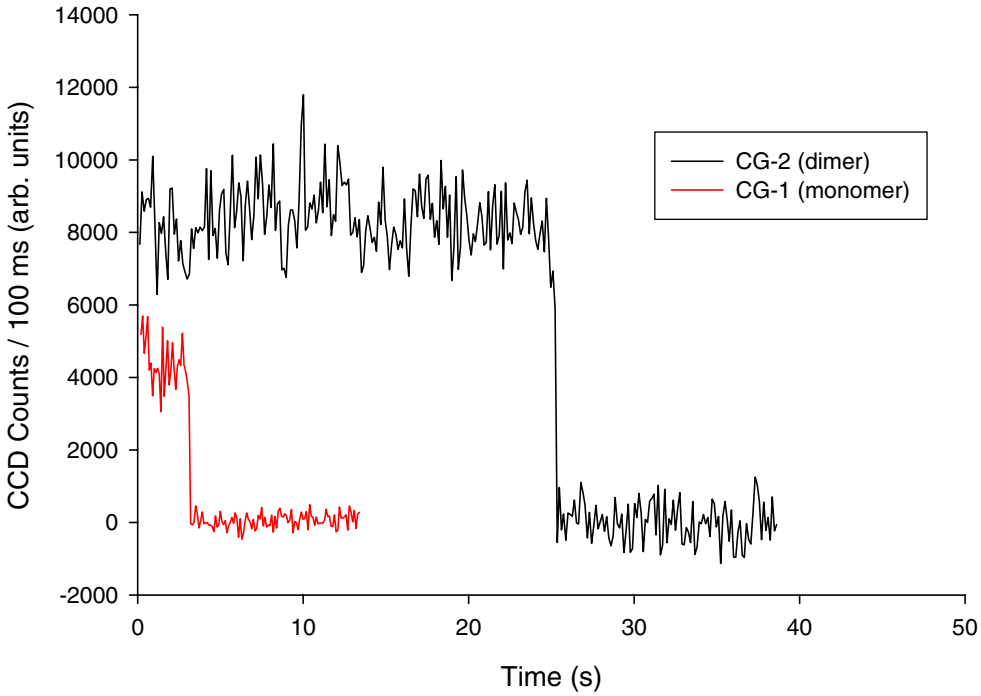

Fig. 8 Single-molecule fluorescence time trajectories for a molecule of CG-2 and a molecule of CG-1 taken under comparable fluorescence imaging conditions

Summary

In this work, the spectroscopic properties of the Ca^{2+} indicator dye CG-1 has been characterized using a combination of ensemble and SM techniques. It was found that the overall increase in fluorescence intensity of this dye with $[Ca^{2+}]_{free}$ can simply be attributed to an increase in number of fluorescent molecules rather than a general increase in the emission intensity of a molecule. Comparison of the absorption spectra for CG-1 and it's dimeric variant, CG-2, allowed for the definitive assignment of a peak in the CG-2 spectrum, further reinforcing the previously proposed mechanism of action. Finally, in a comparison of the two indicator dyes, CG-1 was found to have one half of the emission intensity of CG-2, which is the simple, expected result for a molecule containing half as many fluorophores.

Acknowledgements Funding for this work was provided by the Natural Sciences and Engineering Research Council of Canada and by the University of Saskatchewan. Professor Ron Steer, Dr. Sophie Brunet and the Saskatchewan Structural Sciences Centre are acknowledged for providing access and technical assistance with fluorescence lifetime measurements.

References

1. Weiss S (1999) Fluorescence spectroscopy of single biomolecules. Science 283(5408):1676–1683
2. Moerner WE, Orrit M (1999) Illuminating single molecules in condensed matter. Science 283(5408):1670–1676
3. Moerner WE (2002) A dozen years of single-molecule spectroscopy in physics, chemistry, and biophysics. J Phys Chem B 106 (5):910–927
4. Ambrose WP, Goodwin PM, Jett JH, Van Orden A, Werner JH, Keller RA (1999) Single molecule fluorescence spectroscopy at ambient temperature. Chem Rev 99(10):2929–2956
5. Prodi L (2005) Luminescent chemosensors: from molecules to nanoparticles. New J Chem 29(1):20–31
6. Prodi L, Bolletta F, Montalti M, Zaccheroni N (2000) Luminescent chemosensors for transition metal ions. Coord Chem Rev 205:59–83
7. Czarnik AW (1994) Chemical communication in water using fluorescent chemosensors. Acc Chem Res 27(10):302–308
8. de Silva A, Gunnlaugsson T, Rice T (1996) Recent evolution of luminescent photoinduced electron transfer sensors. Analyst 121:1759–1762
9. Callan JF, de Silva AP, Magri DC (2005) Luminescent sensors and switches in the early 21st century. Tetrahedron 61(36): 8551–8588
10. Zang L, Liu RC, Holman MW, Nguyen KT, Adams DM (2002) A single-molecule probe based on intramolecular electron transfer. J Am Chem Soc 124(36):10640–10641
11. Brasselet S, Moerner WE (2000) Fluorescence behavior of single-molecule pH-sensors. Single Mol 1:17–23
12. Brasselet S, Peterman EJG, Miyawaki A, Moerner WE (2000) Single-molecule fluorescence resonant energy transfer in calcium concentration dependent cameleon. J Phys Chem B 104(15): 3676–3682
13. Ha T, Zhuang XW, Kim HD, Orr JW, Williamson JR, Chu S (1999) Ligand-induced conformational changes observed in single RNA molecules. Proc Natl Acad Sci U S A 96(16):9077–9082
14. Cossart R, Lkegaya Y, Yuste R (2005) Calcium imaging of cortical networks dynamics. Cell Calcium 37(5):451–457
15. Knot HJ, Laher I, Sobie EA, Guatimosim S, Gomez-Viquez L, Hartmann H, Song LS, Lederer WJ, Graier WF, Malli R,

Frieden M, Petersen OH (2005) Twenty years of calcium imaging: cell physiology to dye for. Mol Interv 5(2):112–127
16. Bagh S, Paige MF (2006) Ensemble and single-molecule fluorescence spectroscopy of a calcium-ion indicator dye. J Phys Chem A 110(22):7057–7066
17. Haugland RP (2002) Handbook of fluorescent probes and research products, 9th edn. Molecular Probes, Eugene, OR
18. Tsien R, Pozzan T (1989) Measurement of cytosolic free Ca-2+ with Quin2. Methods Enzymol 172:230–262
19. Tsien RY (1980) New calcium indicators and buffers with high selectivity against magnesium and protons—design, synthesis, and properties of prototype structures. Biochemistry 19(11):2396–2404
20. Grynkiewicz G, Poenie M, Tsien RY (1985) A new generation of Ca-2+ indicators with greatly improved fluorescence properties. J Biol Chem 260(6):3440–3450
21. Minta A, Kao JPY, Tsien RY (1989) Fluorescent indicators for cytosolic calcium based on rhodamine and fluorescein chromophores. J Biol Chem 264(14):8171–8178
22. de Silva AP, Gunaratne HQN (1990) Fluorescent pet (photoinduced electron-transfer) sensors selective for submicromolar calcium with quantitatively predictable spectral and ion-binding properties. J Chem Soc. Chem Commun 2:186–188
23. Bagh S, Paige MF (2005) Construction and application of a single-molecule fluorescence microscope. Can J Chem 83(5):435–442
24. Dickson RM, Norris DJ, Tzeng YL, Moerner WE (1996) Three-dimensional imaging of single molecules solvated in pores of poly (acrylamide) gels. Science 274(5289):966–969
25. Dickson RM, Cubitt AB, Tsien RY, Moerner WE (1997) On/off blinking and switching behaviour of single molecules of green fluorescent protein. Nature 388(6640):355–358
26. Sanders R, Gerritsen HC, Draaijer A, Houpt PM, Levine YK (1994) Fluoresence lifetime imaging of free calcium in single cells. Bioimaging 2:131–138
27. Tessier A, Meallet-Renault R, Denjean P, Miller D, Pansu RB (1999) Conformational dynamics of Calcium Green 1 by fluorescence correlation spectroscopy. PCCP 1:5767–5769
28. Basche T, Ambrose WP, Moerner WE (1992) Optical-spectra and kinetics of single impurity molecules in a polymer–spectral diffusion and persistent spectral hole burning. J Opt Soc Am B 9(5):829–836